Multi-scale (time and mass) dynamics of space objects
Proceedings IAU Symposium No. 364, 2022
A. Celletti, C. Galeş, C. Beaugé, A. Lemaitre, eds.
doi:10.1017/S1743921322000011

Weak stability transition region near the orbit of the Moon

Zoltán Makó and Júlia Salamon

Department of Economic Sciences, Sapientia Hungarian University of Transylvania, Miercurea Ciuc, Romania

Abstract. This paper provides a study on the weak stability transition region in the framework of the planar elliptic restricted three-body problem. We define the lower boundary curve of the weak stability transition region and as a particular case, we determine this curve in the Sun-Earth system. The orbit of the Moon is near the lower boundary of the weak stability transition region.

Keywords. Weak stability boundary; Weak stability transition region; Elliptic restricted three-body problem.

1. Introduction

The capture of small bodies by major planets is an important phenomenon in planetary systems. The phenomenon has applications to the study of comets, asteroids, irregular satellites of the giant planets and different types of low energy planetary transfers, as well.

Ballistic capture (or weak capture) is analytically defined for the n-body problem, and it monitors the sign of the Kepler energy with respect to a massive primary. Weak capture occurs in special regions of the phase space, namely around one of the two primaries (e.g. the Earth in the case of the Sun–Earth system), which are referred to as the Weak Stability Boundaries (WSB). These regions are the boundary of the stable regions, delimiting stable and unstable orbits.

WSB was first introduced by Belbruno (1987) to design low energy transfers to the Moon and it is rigorously defined in Belbruno (2004). García & Gómez (2007) proposed a more general definition, which generalizes the concept of WSB given by Belbruno, and expanded the range of the WSB. The concept of WSB was extended in more accurate models by Belbruno, Topputo & Gidea (2008); Belbruno, Gidea & Topputo (2008); Belbruno, Gidea & Topputo (2013), Topputo & Belbruno (2009), Romagnoli & Circi (2009). Ceccaroni, Biggs & Biasco (2012) gave an analytical definition of the WSB. The effect of primaries' true anomaly on the structure of WSB was treated by Hyeraci & Topputo (2013) and Makó et al. (2010) in the model of elliptic restricted three-body problem (ER3BP).

In these articles, dedicated to the study of WSB properties, certain parameters (for example, the true anomaly of Earth, the initial eccentricity of the test particle, the direction of velocity vector at the initial time of the test particle) are considered constant and the initial position $\mathbf{r}_2$ of the test particle relative to the primary P_2 is considered a variable parameter. The modulus of initial velocity $\mathbf{v}_2(\mathbf{r}_2)$ of the massless particle relative to the primary P_2 is determined, and then the weak stability of the orbit with the initial values $(\mathbf{r}_2, \mathbf{v}_2(\mathbf{r}_2))$ is examined. In these cases, the variable parameter is $\mathbf{r}_2$.

The aim of this article is to study the properties of the transition zone where the weakly stable region switches over to weakly unstable region if $\mathbf{v}_2$ is considered as a variable parameter also. In Section 2 we recall the definition of the WSB. Section 3 contains the definition of the lower boundary curve of weak stability transition region. In Section 4, as a case study, we determine the lower boundary curve of the weak stability transition region around the Earth in the Sun-Earth system in the framework of ER3BP. We compare the position of the boundary curve to the Earth-Moon mean distance and to the radius of the Earth's Hill sphere. The concluding remarks are described in Section 5.

We choose the planar elliptic restricted three-body problem (PER3BP) model to study the dynamics, since even a small change of the eccentricity of the secondary influences the weak stability of the orbits. This model also takes into consideration the weak stability dependence on the true anomaly of the Earth.

In the PER3BP two massive primaries P_1 and P_2, with masses m_1 and m_2 revolve on elliptical orbits under their mutual gravitational attraction. Apart from these two bodies, the motion of a third, massless particle P_3 is investigated. The variation of the distance $R = \|P_1P_2\|$ with respect to the true anomaly f of the primary P_2 is given by $R = a\left(1-e^2\right)/(1+e\cos f)$, where a is the semi-major axis, e is the eccentricity and P is the orbital period of the elliptical orbit of P_2 around P_1. The motion of P_3 is restricted to the orbital plane of the primaries. The mass ratio is $\mu = m_2/(m_1+m_2)$, if $m_1 > m_2$.

The origin O of this system is considered to be the center of mass of the two massive primaries, where the $\tilde{\xi}$ axis is directed towards P_2, and the $\tilde{\xi}\tilde{\eta}$ coordinate-plane rotates with a variable angular velocity, in such a way that the two massive primaries are always on the $\tilde{\xi}$ axis and the period of the rotation is 2π. Beside the rotation, the system also pulsates in order to keep the primaries in fixed positions ($\tilde{\xi}_1 = -\mu$, $\tilde{\eta}_1 = 0$, $\tilde{\xi}_2 = 1-\mu$, $\tilde{\eta}_2 = 0$). To obtain a relatively simple set of equations, we use a nonuniform rotating and pulsating coordinate system (Szebehely (1967)).

To investigate the weak stability, we need a new coordinate system P_2xy, where the center P_2 is continuously moving and the axis P_2x is always parallel with the initial direction of the axis $O\tilde{\xi}$. The connections between these two reference frames are given in (Makó et al. (2010)).

If the normalized units are $a(1-e)=1$ and $2\pi/P=1$, then the Keplerian energy of the massless particle related to P_2 (Makó et al. (2010)) is

$$H_2 = \frac{v_2^2}{2} - \frac{Gm_2}{r_2} = \frac{v_2^2}{2} - \frac{1}{(1-e)^3}\frac{\mu}{r_2} = \frac{(1+e\cos f)^2}{2(1+e)(1-e)^3}\cdot$$
$$\left[\left(\tilde{\xi}' + D(f)\left(\tilde{\xi}+\mu-1\right)-\tilde{\eta}\right)^2 + \left(\tilde{\eta}' + D(f)\tilde{\eta}+\tilde{\xi}+\mu-1\right)^2 - \frac{1}{1+e\cos f}\cdot\frac{2\mu}{\tilde{r}_2}\right],$$

where the derivatives are taken with respect to the true anomaly f of the primary P_2, $D(f) = e\sin f/(1+e\cos f)$, and $\tilde{r}_2 = \sqrt{\left(\tilde{\xi}+\mu-1\right)^2+\tilde{\eta}^2}$.

2. The algorithmic definition of WSB in PER3BP

We recall the construction procedure of WSB introduced by Belbruno (2004) and improved by García & Gómez (2007) and Ceccaroni, Biggs & Biasco (2012).

For a fixed initial value of the true anomaly $f = f_0$ of P_2, we consider the half-line $l(\alpha, f_0)$ starting from P_2 and making an angle $\alpha \in [0, 360^o)$ with the axis P_1P_2 (see Fig. 1). The initial position of P_3 is on $l(\alpha, f_0)$. The initial eccentricity e_3 of the test particle P_3 is fixed. The direction of velocity vector of P_3 at the initial time is perpendicular to the line $l(\alpha, f_0)$. The initial distance between P_2 and P_3 in the coordinate system P_2xy is r_2 and the semi-major axis is $a_3 = r_2/(1-e_3)$.

https://doi.org/10.1017/S1743921322000011 Published online by Cambridge University Press

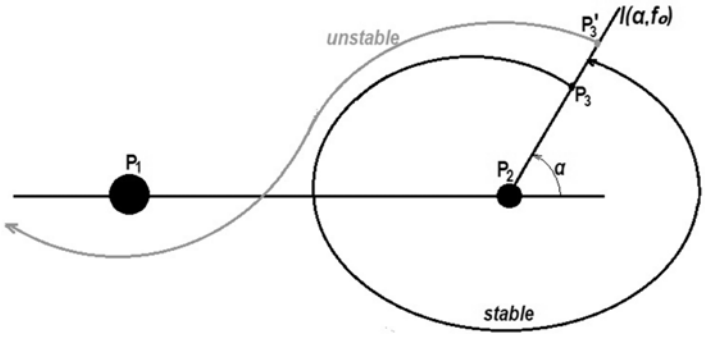

Figure 1. Construction procedure of WSB.

The modulus of velocity vector of P_3 at the initial time with respect to the reference frame P_2xy is

$$v_2^2\left(r_2,e_3\right)=\frac{Gm_2\left(1+e_3\right)}{r_2}=\frac{\mu\left(1+e_3\right)}{\left(1-e\right)^3\cdot r_2}\in\left[v_c^2\left(r_2\right),v_e^2\left(r_2\right)\right],$$

where $v_c\left(r_2\right)=v_2\left(r_2,0\right)$ is the circular initial velocity and $v_e\left(r_2\right)=v_2\left(r_2,1\right)$ is the escape initial velocity with respect to primary P_2 in the context of the two-body problem.

We transform the initial position $(r_2\cos\alpha, r_2\sin\alpha)$ and initial velocity $\pm(-v_2\sin\alpha, v_2\cos\alpha)$ of P_3 (+ for direct, − for retrograde direction) from reference frame P_2xy into the reference frame $O\tilde{\xi}\tilde{\eta}$, where $(\tilde{\xi}_0,\tilde{\eta}_0)$ is the initial position and $(\tilde{\xi}_0',\tilde{\eta}_0')$ is the initial velocity of P_3 given by formulas (7) and (9) in Makó et al. (2010).

The motion of a particle is said to be weakly stable relative to P_2, under the PER3BP dynamics, if after leaving $l(\alpha,f_0)$ the particle P_3 makes a full cycle around P_2 without going near to P_1 or crashing into P_2 and returns to a point on $l(\alpha,f_0)$ with Kepler energy $H_2\left(\gamma\left(T\right)\right)\le 0$ at the first return time T to half-line $l(\alpha,f_0)$. Otherwise, the motion will be weakly unstable.

García & Gómez (2007) show, that for each fixed $(\alpha,e_3)\in[0^o,360^o)\times[0,1)$ there are many changes from weak stability to weak instability and that the set of weakly stable points is a Cantor set.

The García & Gómez (2007) definition of WSB in the PER3BP model, taking into consideration Ceccaroni, Biggs & Biasco (2012) is the following.

Definition 1. For all fixed $(f_0,\alpha,e_3)\in[0^o,360^o)\times[0^o,360^o)\times[0,1)$ we set

$$\begin{aligned}S^*\left(f_0,\alpha,e_3\right)=\{&r_2>0:\text{ the orbit of test particle with initial condition}\\&\left(\mathbf{r}_2,\mathbf{v}_2\left(\mathbf{r}_2,e_3\right)\right)\text{ is weakly stable and the angular velocity }\dot{\vartheta}\left(T\right)>0\\&\text{at the first return time }T\text{ to half-line }l(\alpha,f_0)\}.\end{aligned}$$

Then the WSB for fixed value of $f_0\in[0^o,360^o)$ and $e_3\in[0,1)$ is defined as:

$$W\left(f_0,e_3\right)=\left\{\left(r_2\cos\alpha,r_2\sin\alpha\right)\in\mathbb{R}^2:\alpha\in[0,360^o)\text{ and }r_2\in\partial S^*\left(f_0,\alpha,e_3\right)\right\}.$$

The WSB lies in the transition zone from the connected part of the weakly stable region to the connected part of the weakly unstable region.

Definition 2. The weak stability transition region (WSTR) is the transition zone from the connected part of the weakly stable region to the connected part of the weakly unstable region in the fixed reference frame P_2xy.

https://doi.org/10.1017/S1743921322000011 Published online by Cambridge University Press

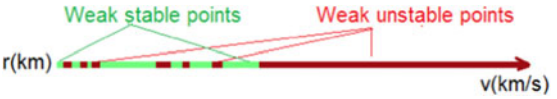

Figure 2. Stable and unstable points for a given true anomaly f_0 and distance r_2 with respect to the value of initial velocities in the system P_2xy.

3. The lower boundary curve in the weak stability transition region

Let f_0 and e_3 be given, and α, r_2 be the variable parameters. In the procedure of constructing the WSB, first, we calculate $v_2\,(r_2, e_3)$, the magnitude of the velocity and then we examine the weak stability of trajectories for initial values $(\mathbf{r}_2, \mathbf{v}_2\,(\mathbf{r}_2, e_3))$. In this case, the variable parameter is r_2.

The question is: what are the properties of WSTR if v_2 is a variable parameter and belongs to an interval $\left[v_2^{\min}(r_2), v_2^{\max}(r_2)\right]$?

For a given r_2, the smallest value of v_2 is $v_2^{\min}\,(r_2)$. In Fig. 2 it can be observed that for a given true anomaly f_0 and distance r_2, as the velocity increases, the orbits are weakly stable for a while (green dots), and after reaching a certain value, the orbits become weakly unstable (red dots). We can also observe that neither the weakly stable domain nor the weakly unstable domain are connected. By increasing the velocity, in the weakly stable region, they will appear weakly unstable parts.

We observe the following property of the WSTR (see Fig. 2).

Property A: There exist distances r_2 from P_2, such that the maximum velocity where the orbit remains weakly stable is strictly larger than the smallest velocity where the orbit becomes weakly unstable.

Next, for a fixed real anomaly f_0, we define the lower boundary curve of WSTR in the P_2xy coordinate system.

Definition 3. The lower boundary curve $LB\,(f_0)$ of the WSTR is

$$LB\,(f_0) = \big\{(r_2^* \cos\alpha, r_2^* \sin\alpha) \in \mathbb{R}^2 : \alpha \in [0^o, 360^o) \text{ and } r_2^* \text{ is the smallest distance from } P_2 \text{ on half-line } l(\alpha, f_0), \text{ where property A appears}\big\}.$$

For a fixed value of f_0, the defined set $LB\,(f_0)$ is two dimensional in WSTR, and it has two components corresponding to the direct and retrograde motions.

The Hill sphere (or Roche sphere) of primary P_2 is the region where the gravitational attraction of P_2 dominates. In the model of PER3BP, with normalized unit $a\,(1-e)=1$, the radius of the Hill sphere of primary P_2 can be approximated (Hamilton & Burns (1992)) by $R_{P_2} = \sqrt[3]{\mu/\,[3\,(1-\mu)]}$. The Hill circle HB around P_2 is

$$HB = \big\{(R_{P_2} \cos\alpha, R_{P_2} \sin\alpha) \in \mathbb{R}^2 : \alpha \in [0^o, 360^o)\big\}.$$

4. Case study for Sun-Earth system

In this section, we investigated the weak stability in the PER3BP model of the Sun-Earth system. For the Sun-Earth system, the mass ratio is $\mu = 3.003158242 \cdot 10^{-6}$ and the eccentricity of the elliptical orbit of Earth is $e = 0.0167$.

First, we classify the weak stability of the orbits based on the initial distance r_2 and initial velocity v_2, where $f_0 = 0^o$ and $\alpha = 45^o$ (Fig. 3). The initial velocities are directly guided. Initial conditions for weakly unstable orbits are marked with red, the initial values for weakly stable orbits with green. The yellow points give the initial values of the collision orbits with the Earth (the trajectories where the distance between the massless particle and Earth will be equal to the radius of the Earth at some time: $\|P_3P_2\| = R_E = 6378$ km). The second panel of Fig. 3 is an enlarged part of the first panel.

https://doi.org/10.1017/S1743921322000011 Published online by Cambridge University Press

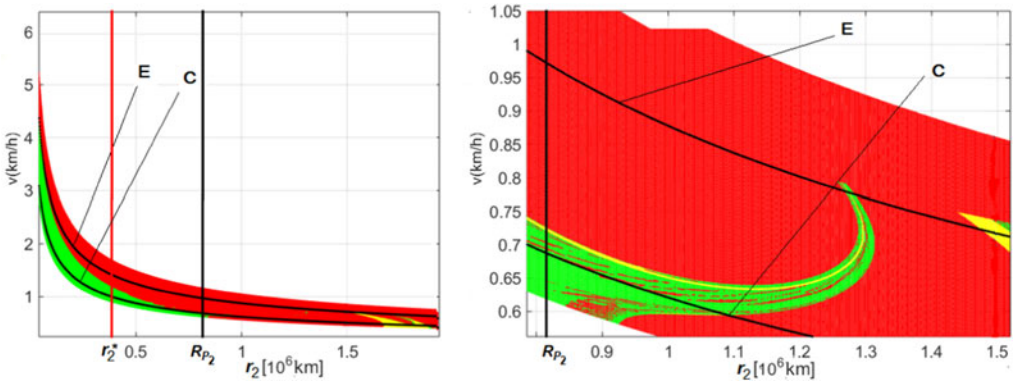

Figure 3. Weak stability in system (r_2, v_2). Initial values for weakly unstable orbits are marked with the color red, the initial values for weakly stable orbits with the color green. The yellow points give the initial values of the collision orbits with the Earth. The second panel is the enlarged part of the first panel.

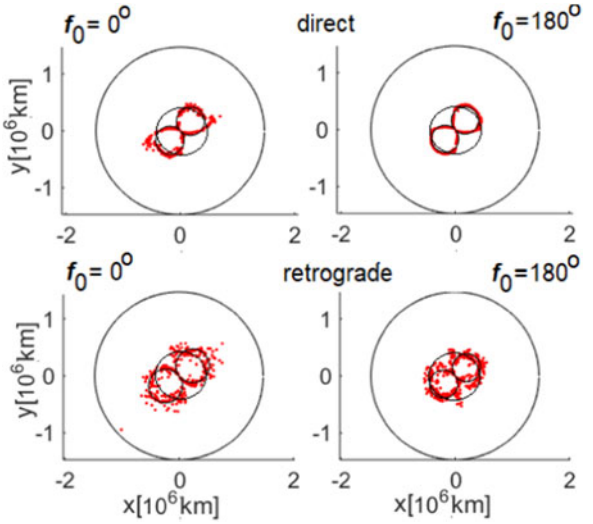

Figure 4. The lower boundary curve of WSTR in the Sun-Earth system for direct and retrograde initial velocities in P_2xy coordinate system, where $f_0 \in \{0^o, 180^o\}$. The points of $LB(f_0)$ are marked by color red. The inner circle is the orbit of the Moon and the outer circle plots the Hill circle. The curve near the red dots shows the best fitting lemniscate.

The two black curves represent the circular (C) and escape (E) velocity for a given distance in two body problem regarding to the planet Earth. The first vertical line (red line) indicates the position of boundary point corresponding to the angle $\alpha = 45^o$ of $LB(0^o)$. At this distance r_2^*, the property A appears for the first time. The second vertical line indicates the position corresponding to the radius of the Hill sphere.

Fig. 4 illustrates the lower boundary curve $LB\,(f_0)$ in coordinate system P_2xy, when $f_0 \in \{0^o, 180^o\}$ and the initial conditions give direct or retrograde motions. The points of $LB(f_0)$ are marked by color red. The inner circle is the orbit of the Moon and the outer circle plots the Hill circle.

Remark 4. In Fig. 4 it can be observed, that the approximation of the lower boundary curve in analytical form can be obtained by fitting a quadratic plane curve to the determined points (red dots). Moreover, in the case of direct motion, the red dots are more

https://doi.org/10.1017/S1743921322000011 Published online by Cambridge University Press

Table 1. The optimal fitting parameters

	f_0	L	L *inf*	L *sup*	L *width*	δ	δ *inf*	δ *sup*	δ *width*
D.	0^o	495318	483949	506538	22589	42.78	41.48	44.08	2.6
D.	180^o	476020	468690	483500	14810	43.11	42.22	44	1.78
R.	0^o	590462	574605	606320	31715	36.44	34.91	37.97	3.06
R.	180^o	490681	476020	505491	29471	35.78	34.06	37.5	3.44

dispersed for $f_0 = 0^o$ than for $f_0 = 180^o$. In the case of retrograde motion, the boundary curves become blurred (with greater dispersion). The points of the $LB\,(f_0)$ are very important in the design of ballistic escape trajectories in the Sun-Earth system. In the graph of direct motion on Fig. 4, we observe weakly unstable points (red dots) around the Moon's orbit in the vicinity of $\alpha = 45^o$.

The $LB(f_0)$ is approximated by a Bernoulli lemniscate (Fig. 4). Thus, an analytical formula is obtained to estimate the lower bound of WSTR. If we fit the lemniscate of Bernoulli : $r^2 = L^2\cos^2(\alpha - \delta)$ to the points of $LB(f_0)$ then we obtain the optimal fitting parameters reported in Tab. 1. When d is the half-distance between the focal points F_1 and F_2 of the lemniscate then $L = d\sqrt{2}$. The δ is the angle between the line F_1F_2 and axis Ox.

The first column of Table 1 indicates that the motion is direct (D.) or retrograde (R.). In the second column the value of the true anomaly and in the third column the length (L[km]) of the best-fitting lemniscate are given. The fourth and fifth columns give the upper and lower limits of the confidence interval of L at a 95% confidence level. The sixth column gives the width of the confidence interval in km.

The seventh column gives the angle $\delta[^o]$ between the semi major-axis of the lemniscate and the axis Ox. The eighth and ninth columns represent the upper and lower limits of the confidence interval of δ at 95% confidence level. The last column gives the width of the confidence interval of δ in degrees.

5. Concluding remarks

In this paper, the velocity is also considered as a variable parameter in the study of weak stability. The lower boundary curve is defined in the weak stability transition-region (WSTR). As an application, the lower boundary curve of WSTR is numerically determined in the PER3BP model of the Sun-Earth system. The location of the lower boundary curve is compared to the Earth-Moon mean distance. We show that the lower boundary curve can be approximated by a Bernoulli lemniscate.

The analysis shows that, if we ignore the mean inclination of Moon's orbit from the ecliptic ($i = 5.15^o$), the orbit of the Moon is near to the lower boundary of the WSTR in the system P_2xy (the first two panel of Fig. 4). The orbit of the Moon intersects $LB\,(f_0)$ at four points, approximately: $\alpha_1 = 41^0$, $\alpha_2 = 45^0$, $\alpha_3 = 221^0$, $\alpha_4 = 225^0$. If the true anomaly of the Moon relative to Earth is approximately in $[41^0, 45^0] \cup [221^0, 225^0]$, then the Moon is below the lower boundary of the WSTR (i.e. the motion is weakly stable), otherwise, it is in the weak stability transition region.

Another interesting situation is when the angle between the directions of Sun-Earth and Earth-test particle is 135^o. In this case, the weakly unstable points are very close to Earth. From these points escape trajectories can be designed even if the initial velocity is smaller than the escape velocity.

The simplicity and enough precise estimation of the lower boundary curve raises the question on whether the equation of the lower boundary curve can be analytically derived in the ER3BP or CR3BP model.

https://doi.org/10.1017/S1743921322000011 Published online by Cambridge University Press

References

Belbruno, E. 1987, in *Proc. of AIAA/DGLR/JSASS Inter. Propl. Conf.* AIAA paper No. 87-1054
Belbruno, E., 2004, *Capture Dynamics and Chaotic Motions in Celestial Mechanics*, Princeton Univ. Press
Belbruno, E., Topputo, F., & Gidea, M. 2008, *Adv Space Res*, 42, 1330
Belbruno, E., Gidea, M., & Topputo, F. 2010, *SIAM J Appl Dyn Syst*, 3, 1061
Belbruno, E., Gidea, M., & Topputo, F. 2013, *Qual Theor Dyn Syst*, 12, 53
Ceccaroni, M., Biggs, J., & Biasco, L. 2012, *Celest Mech Dyn Astr*, 114, 1
García, F., & Gómez, G. 2007, *Celest Mech Dyn Astr*, 97, 87
Hamilton, D.P., & Burns, J.A. 1992, *Icarus*, 96, 43
Hyeraci, N., & Topputo, F. 2013, *Celest Mech Dyn Astr*, 116, 175
Makó, Z., Szenkovits, F., Salamon, J., & Oláh-Gál, R. 2010, *Celest Mech Dyn Astr*, 108, 357
Romagnoli, D., & Circi, C. 2009, *Celest Mech Dyn Astr*, 103, 79
Szebehely, V. 1967, *Theory of orbits*, Academic Press, New-York
Topputo, F., Belbruno, E. 2009, *Celest Mech Dyn Astr*, 3, 17

https://doi.org/10.1017/S1743921322000011 Published online by Cambridge University Press